Tackling polypharmacology of kinase inhibitors and selecting chemical kinase probes by transcription factor activity profiling.

Alexander V. Medvedev[1], Sergei Makarov Jr. [1], Lyubov A. Medvedeva[1], Elena Martsen[1], Kristen L. Gorman[1], Benjamin Lin[1], Sergei S. Makarov[1,*].

[1]Attagene Inc., 7020 Kit Creek Rd, Morrisville NC 27560

*Corresponding author

smak@attagene.com

tel 919-270-6031

ABSTRACT.

Protein kinase inhibitors (PKI) evolved as promising drugs for multiple diseases. However, PKIs' promiscuity causes polypharmacological effects challenging therapeutic development. We show that the polypharmacology of PKIs can be inferred from their impact on transcription factors (TF) lying at the apexes of signaling pathways. Using a high-content reporter assay, we evaluated TF activity profiles (TFAP) in cells treated with Akt, CDK, Aurora, Raf, MEK, and ERK inhibitors. For each kinase family, we found kinase-specific consensus TFAP signatures signifying the on-target PKI activity. Remarkably, proximal kinases had the highest similarity of their PKIs' consensus signatures. Furthermore, we show that individual PKIs exhibited the consensus, "on-target signatures" within certain "specificity windows" and distinct "off-target signatures" at other concentrations. We also show that the TFAP signatures permit pinpointing the off-target PKI activity at irrelevant kinases and non-kinase effectors. Therefore, the TFAP approach provides clear-cut quantitative metrics for assessing PKI activity and concentration ranges where the on-target activity dominates cell response. By illuminating PKI biology invisible to target-based techniques, this effect-based approach streamlines the selection of kinase chemical probes and PKI drug prioritization.

INTRODUCTION.

Protein kinases are considered by many as the most important drug targets for cancer[1,2], and kinase drug discovery is rapidly expanding into immunological, inflammatory, degenerative, metabolic, cardiovascular, and infectious diseases[3]. One of the most challenging issues in therapeutic development is PKI promiscuity stemming from a significant homology of the active kinase centers[4,5]. Genome-wide profiling studies revealed that even the ‘selective’ PKIs act on multiple kinases[4,6–8]. Furthermore, like other drugs, PKIs can interact with a plethora of non-kinase effectors, such as bromodomain-containing proteins, cytoskeleton, prostaglandin synthases, the AHR receptor, ferrochelatase, and NQO2[9].

The polypharmacological effects of multiple PKI interactions pose difficult questions to drug developers. On the one hand, PKI polypharmacology can compromise drug safety, but it can also increase the therapeutic efficacy[10]. Furthermore, it complicates the selection of selective chemical probes needed for elucidating the kinases’ functions and target validation. The existing PKI evaluation techniques are focusing on profiling the PKI binding/inhibitory activity across kinases; however, these target-based approaches do not provide clear guidance for prioritizing drug candidates and chemical probe selection.

Here, we present an orthogonal, effect-based approach evaluating the biological effects of PKIs. This approach entails assessing PKIs’ impact on the cellular network of signal transduction pathways that regulate gene expression. As a readout, we evaluate the activity of transcription factors (TFs) that link signaling pathways to regulated genes. Thus, by profiling TFs’ activity we can capture the activation status of the cellular signaling network.

Our approach is based on the premise that protein kinases lie at the heart of signal transduction pathways. Furthermore, as we demonstrated previously, perturbagens of various biological processes and cell systems cause coordinated changes in the activity of signaling pathways, epitomized by specific TF activity profiles (TFAP)[11].

Thus, we sought to determine if cells' response to kinase inhibitors, too, can be described by specific TFAP signatures. To do that, we examined the TFAP signatures for inhibitors of Akt, Aurora, cyclin-dependent kinases (CDKs), Raf, MEK, and ERK kinase families. For this purpose, we used our high-content reporter assay (the FACTORIAL®) enabling a parallel evaluation of multiple TFs in a single well of cells[12].

We found that different inhibitors of each kinase family, regardless of their mode of action (ATP-competitive or allosteric), shared a distinct consensus TFAP signature. Using the TFAP signatures permitted assessing the on-target and off-target PKI activity, and the concentration ranges where these activities dominate. Furthermore, we show that this approach enables a straightforward solution to selecting chemical probes for kinases. Thus, the effect-based TFAP approach complements the existing, target-based techniques to streamline the development of chemical probes and kinase drug prioritization.

RESULTS.

Profiling TF activity by the FACTORIAL assay. The FACTORIAL is a high-content reporter assay enabling a parallel assessment of multiple TFs in a single well of cells[13]. The assay comprises a set of TF-responsive reporters termed reporter transcription units (RTUs). The RTUs are largely identical to traditional reporter gene constructs, but their activity is evaluated by detecting the reporter RNA transcripts.

The assay workflow entails transient transfection of RTU plasmids into assay cells followed by profiling RTU transcripts. A homogeneous design of the FACTORIAL enables equal detection efficacy across RTUs, which drastically reduces the influence of experimental variables and ensures exceptionally robust and reproducible TF activity profiles (TFAP)[13] (Fig. S1).

The endpoints of FACTORIAL-generated TFAP signatures encompass TF responses to various stimuli, including xenobiotics, growth factors, inflammation, and various stresses (listed by Fig. S1).

Assessing PKI TFAP signatures. The TFAP signatures of PKIs are presented here as radial graphs showing TF activity fold-change in drug-treated vs. vehicle-treated cells. By this definition, the TFAP signature of vehicle-treated cells is a perfect circle (the "null" signature). Each presented here TFAP signature is an average of three independent FACTORIAL assays.

To assess the pair-wise similarity of TFAP signatures, we use Pearson correlation coefficient ***r***. The signatures with the similarity $r>0.70$ are considered identical because the probability of two random 47-endpoint signatures correlating with $r> 0.70$ is extremely low ($P<10^{-7}$)[14].

Here, we evaluated signatures of a diverse panel of inhibitors of Akt, cyclin-dependent kinases (CDK), Aurora, Raf, MEK, and ERK kinase families. Each PKI was evaluated in a concentration-response format, in a broad concentration range. To find a consensus signature shared by different inhibitors of a given kinase family, we analyzed their TFAP signatures at different concentrations by a cluster analysis, seeking for the signature cluster encompassing most of PKIs.

The consensus signature of AKT inhibitors. The Akt1, Akt2, and Akt3 kinases mediate cell responses to various stress stimuli and growth factors. This kinase family plays a critical role in multiple cellular processes such as glucose metabolism, apoptosis, cell proliferation, and migration[15]. Furthermore, Akt kinases play a prominent role in cancer[15], which prompted the development of anticancer Akt inhibitors[16,17].

The analysis of four ATP-competitive pan-Akt inhibitors and one allosteric Akt 2/3 inhibitor (Fig. 1A) revealed a tight signature cluster that included each inhibitor. The signatures of individual inhibitors matched the center cluster signature (i.e., the consensus TFAP signature) at multiple concentrations (Fig. 1A, see also Fig. S2 for more data). In addition, expressing a kinase-dead Akt mutant (Akt K179M) cDNA also produced the consensus Akt PKI signature (Fig. 1A). Therefore, regardless of the mode of action and their targets within the Akt family, Akt inhibitors produced identical signatures.

Furthermore, individual endpoints of the Akt PKI consensus signature were consistent with known TFs targets of Akt (β-catenin/TCF[18], IRFs[19], NF-κB[20], and p53[21]). These data, combined, suggest the consensus signature as a specific marker for the on-target Akt PKI activity.

The consensus signature of CDK inhibitors. The family of cyclin-dependent kinases (CDK) comprises multiple kinases that control different cell cycle stages and are also involved in regulating mRNA transcription and processing. Due to the critical role of CDKs in cell proliferation, CDK inhibitors have been developed for multiple cancers[22].

Cluster analysis of 13 CDK inhibitors (listed by Fig. 1B) with different selectivity profiles revealed a consensus signature matching individual inhibitors' signatures at multiple concentrations (Fig. 1B, see also Fig. S3A for more inhibitors' data). Therefore, CDK inhibitors had a consensus signature, regardless of their specific kinase targets within the CDK family.

The consensus signature of Aurora inhibitors. Aurora kinases A, B, and C play a crucial role in cellular division by controlling chromatid segregation, making this kinase family an anticancer drug target[23]. The TFAP evaluation of five Aurora ATPase inhibitors (Fig. 1C) showed that inhibitors with different selectivity profiles had a consensus signature (Fig. 1C and Fig. S4), regardless of their targets within the Aurora family.

The consensus signatures of Raf, MEK, and ERK inhibitors. Mitogen-activated protein kinase (MAPK) cascades regulate cell proliferation, survival, and differentiation. The extracellular signal-regulated kinase (ERK) MAPK pathway is considered a particularly important player in oncogenesis[24].

The ERK MAPK pathway constitutes Raf kinases that phosphorylate and activate downstream MAPK/ERK kinases (MEK)1/2 that, in turn, activate ERK1/2 kinases. An important role for the Raf/MEK/ERK cascade in oncogenesis is evidenced by mutational activation of Raf in many cancers[25]. Additionally, the Raf/MEK/ERK pathway is a key downstream effector of the Ras GTPase, the most frequently mutated oncogene in human cancers[24,25].

Testing the panel of five pan-Raf inhibitors and two B-Raf inhibitors revealed a consensus TFAP signature (Fig. 2A, see also Fig. S5). Furthermore, inhibitors of the downstream MEK1/2 and ERK1/2 kinases also showed distinct consensus signatures (Fig. 2B,C and

Fig. S6). The endpoints of these signatures were consistent with known TF targets of the Raf/MEK/ERK pathway, e.g., AP-1[24] and NRF2[26].

The similarity of consensus PKI signatures correlates with the proximity of their targets. Next, we analyzed the similarity of the consensus PKI signatures for different kinase families. The highest similarity values were found for the proximal kinases of the Raf/MEK/ERK cascade (Fig. 3), In fact, the pairwise similarity values of the consensus Raf, MEK, and ERK PKI signatures exceeded the identity threshold (r>0.70). in contrast, distant kinases (CDK, Aurora, and Akt) had a low-degree similarity (Fig. 3).

Examining polypharmacology of individual PKIs. Our data showed that the TFAP signatures of individual PKIs matched the consensus PKI signature only within certain concentration ranges that we termed the "specificity windows". At other concentrations, we observed distinct, "off-target signatures". To assess the underlying off-target activities, we queryied our TFAP database of reference perturbagens, as exemplified by Figs. 4-6.

CDK inhibitors. Fig. 4 shows TFAP signatures of CDK inhibitors Dinaciclib and NU6140. Dinaciclib inhibits CDK2, CDK5, CDK1, and CDK9 kinases with nanomolar IC50 values in a cell-free assay[27]. NU6140 was developed as a selective CDK2 inhibitor with IC50 of 0.4 uM[28].

Dinaciclib's signature matched the consensus CDK PKI signature at all tested concentrations (30 nM to 20 uM) (Fig. 4A). In contrast, NU6140 showed the consensus CDK PKI signature only at one concentration (6.7 uM); at lower concentrations, its signatures matched the consensus signature of Aurora inhibitors (Fig. 4B). Therefore, cell response to NU6140 at low concentrations was dominated by Aurora inhibition, and CDK inhibition at higher concentrations. These data were consistent with a high affinity of NU6140 to Aurora A/B kinases (IC50 of 67 and 35 nM, respectively)[29].

Akt inhibitors. Fig. 5 shows TFAP signatures of Akt inhibitors GDC0068 and A674563. GDC-0068 (a.k.a. Ipatasertib and RG7440) is a pan-Akt inhibitor targeting Akt1/2/3 with IC50 of 5 nM/18 nM/8 nM in cell-free assays[30]. A674563 is a multi-kinase inhibitor of Akt1 (IC50 of 11 nM in cell-free assays), PKA, Cdk2 (IC50 of 16 nM and 46 nM)[31], and FLT3 (IC50=2.1 uM)[32].

The GDC-0068 showed the consensus Akt PKI signature at all tested concentrations (60 nM to 15 uM) (Fig. 5A). In contrast, A674563 signatures were dissimilar to the Akt PKI consensus signature but had a high similarity to the consensus CDK PKI signature (Fig. 5B). Therefore, cells' response to GDC-0068 was shaped by Akt inhibition, whereas the dominant biological effect of A674563 stemmed from CDK inhibition.

ERK inhibitors. Fig. 6 shows TFAP signatures of ATP-competitive ERK inhibitors GDC-0094 and Ulixertinib. GDC-0994 (a.k.a. Ravoxertinib) is an ERK1/2 inhibitor with IC50 of 1.1 nM and 0.3 nM, respectively[33]. Ulixertinib (BVD-523; VRT752271) is a reversible ERK1/2 inhibitor with IC50 of <0.3 nM at ERK2 also inhibiting RSK kinase[34].

GDC-0994 elicited the consensus ERK PKI signature at concentrations ranging from 30 nM to 2.2 uM (Fig. 6A). However, at a higher concentration (6.7 uM), the GDC-0994 signature had a high similarity to the consensus TFAP signature of histone deacetylase (HDAC) inhibitors[11].

Ulixertinib showed identical to the consensus ERK PKI signature at concentrations from 30 nM to 250 nM (Fig. 6B). At the concentration of 2.2 uM, the Ulixertinib signature had a higher similarity to the Raf PKI consensus signature; at 6.7 uM, it matched the consensus TFAP signature of mitochondria inhibitors[11].

Therefore, the TFAP signatures suggested that, beyond the specificity window, GDC-0994 had an off-target activity at HDAC, whereas Ulixertinib inhibited mitochondria function. The latter prediction was tested and confirmed by a cell-based mitochondria function assay (Fig. S7). That suggests that the TFAP approach permits assessing the off-target PKI activity at non-kinase effectors.

Evaluating PKIs as chemical probes. A chemical kinase probe is a selective small-molecule modulator of kinase activity. These probes are indispensable for delineating the mechanistic and phenotypic effects of kinases in cell-based and animal studies and for drug target validation[35–37]. Chemical probes must be active in cells and satisfy other quality criteria, such as selectivity and chemical stability[35,37,38]. Another essential parameter is the concentration range wherein cell response is primarily shaped by the probe's specific activity toward the target kinase.

The TFAP approach offers a straightforward solution for selecting chemical kinase probes. Since inhibitors of the same kinase family, regardless of their MOA, have identical signatures, we consider the PKI consensus signatures as bona fide markers for the on-target PKI activity. Since the individual inhibitors elicit the consensus PKI signatures only within certain ‘specificity windows’, these windows define the appropriate concentration ranges for chemical probes.

To illustrate this evaluation approach, we compared concentration-dependent signatures of Akt and MEK inhibitors to their consensus PKI signatures (Fig. 7). Among Akt inhibitors, GDC-0068 matched the consensus Akt PKI signature ($r>0.70$) in the largest concentration range (Fig. 7A). Among MEK inhibitors, Binimetinib and Selumetinib showed the largest specificity windows (Fig. 7B). Notably, our data agree with the Chemical Probes Portal also proposing Selumetinib as a chemical probe for MEK[39]. Therefore, TFAP-based evaluation provides clear-cut criteria for selecting chemical kinase probes.

DISCUSSION.

In this work, we have described an effect-based evaluation approach that entails profiling PKI effects on cellular signaling. As the readout, we assessed the activity of transcription factors that connect the signaling pathways to regulated genes. Using a high-content reporter assay (the FACTORIAL), we characterized cell response by quantitative signatures (TF activity profiles). We examined the PKI TFAP signatures at a late (24 h) time point to obviate PKI's transient effects and different pharmacokinetics. The main findings are as follows:

1. We found that different Inhibitors of the same kinase, regardless of their mode of action, elicited identical TFAP signatures at certain concentrations. An example is the consensus signature of ATP-competitive and allosteric Akt inhibitors and the kinase-dead Akt mutant (Figs. 1A and S2). That indicates that kinase inhibition causes specific coordinated changes in signaling pathways' activity, epitomized by the consensus PKI signatures. Thus, the consensus signatures appear bona fide markers for PKIs’ on-target activity.

2. We found kinase-specific PKI consensus signatures for CDK, Aurora, Raf, ERK, and MEK (Figs. 1-2), indicating that such PKI TFAP signatures should also exist for many other kinases in the human kinome.

3. We found high-similarity PKI consensus signatures for proximal kinases of the same kinase cascade (Raf/MEK/ERK), distinguishing them from distal kinases (Fig. 3). This observation further supports the consensus PKI signatures as the on-target activity markers. Furthermore, these data suggest that PKI consensus signatures may help placing poorly characterized "dark kinases" into the framework of the illuminated kinome.

4. Individual PKIs' signatures matched the consensus PKI signature only within certain concentration ranges (Figs. 4-8), suggesting that cells' response to a PKI within the 'specificity window' is defined by its on-target activity. At other concentrations, we observed distinct signatures indicating off-target PKI activities. What is essential, querying the TFAP signatures of reference perturbagens allowed identifying the underlying off-target activity. Therefore, the TFAP approach generates clear quantitative metrics (the consensus, on-target PKI signature, the specificity window, and the off-target signatures) for PKI bioactivity assessment.

One important application of the TFAP approach is for evaluating chemical probes for kinases. We showed that concentration-response TFAP assessments provided clear-cut criteria for selecting appropriate concentration ranges for chemical probes (Fig. 7). Moreover, as TFAP signatures are obtained after a prolonged PKI incubation in assay cells, our approach also addresses other essential probe parameters, i.e., activity in cells, biotransformation, and chemical stability.

Another application of the TFAP approach is the evaluation of kinase drug candidates. The PKI polypharmacology can compromise drug safety, but it can also significantly potentiate therapeutic efficacy[10]. In this regard, our approach allows assessing PKI concentrations for the on-target PKI activity and off-target effects on irrelevant kinases and non-kinase effectors.

Previously, we showed characteristic TFAP signatures for perturbations of various biological processes and cell systems, including inhibitors of mitochondria function and Ub/PS protein degradation pathway, histone deacetylation, DNA damaging agents, and cytoskeleton disruptors[11]. The present work expands this list by the characteristic TFAP signatures for kinase inhibitors. Therefore, the TFAP-based evaluation is a general approach for a comprehensive biological evaluation of uncharacterized compounds.

A distinct advantage of the TFAP approach is that it operates with reproducible quantitative signatures and thus permit directly comparing compounds' bioactivity without complicated bioinformatic analyses needed by other systems biology approaches (e.g., transcriptomics).

One caveat of our evaluation approach is that proximal kinases have high-similarity signatures. Because of that, our FACTORIAL assay may not have sufficient resolution to distinguish inhibitors of some kinases. In this regard, the assay resolution can be increased by expanding the FACTORIAL by additional TF reporters. Another limitation is that TFAP signatures allow distinguishing inhibitors of different kinase families but not specific kinase targets. Therefore, a comprehensive PKI evaluation should involve PKI selectivity profiling by orthogonal, target-based techniques[5,6].

In summary, the effect-based TFAP approach illuminates PKI biology invisible to existing target-based evaluation techniques. That expands the kinase research toolbox, facilitating chemical kinase probe evaluation and drug development.

FIGURE LEGENDS.

Fig. 1. The consensus TFAP signatures of Akt (A), CDK (B), and Aurora (C) inhibitors. The PKIs (*left panels*) were evaluated by the FACTORIAL assay in human hepatocyte HepG2 cells in a concentration-response format (a 24-h incubation). Each TFAP signature is an average of three independent FACTORIAL assays. The PKI TFAP signatures were analyzed by unsupervised hierarchical cluster analysis to identify the consensus signatures. The similarity values for the consensus and individual PKI signatures were calculated as the Pearson correlation coefficient ***r*** (*left panels*). The *central panels* show the consensus PKI signatures (in blue) overlaid by the signatures of individual PKIs (in red). The TFAP signatures' axes show fold-change TF activity values in PKI-treated vs. vehicle-treated cells (on a log scale). *The right panel:* The TFAP signatures' endpoints (see supplementary Fig. S1 for a detailed description).

Fig. 2. The consensus TFAP signatures of Raf (A), MEK (B), and ERK (C) inhibitors. The PKIs were evaluated as described by Fig. 1 legend.

Fig. 3. The similarity of consensus PKI signatures correlates with kinases' proximity. The clustering tree shows the similarity values for the consensus PKI signatures of indicated kinases. The signatures were analyzed by unsupervised hierarchical cluster analysis. The similarity of the signatures calculated as Pearson correlation coefficient ***r***.

Fig. 4. The TFAP-based assessment of CDK inhibitors' polypharmacology. The PKIs' TFAP signatures were obtained as described by Fig. 1 legend. **A.** The TFAP signatures of Dinaciclib (in red) at indicated concentrations overlayed on the consensus CDK PKI signature (in blue). **B.** The TFAP signatures of NU 6140 (in red) at indicated concentrations overlayed on the consensus CDK (upper panel) and Aurora (bottom panel) PKI signatures. The similarity of the overlaid signatures calculated as Pearson correlation coefficient ***r***. Each TFAP signature is an average of three independent FACTORIAL assays.

Fig. 5. The TFAP-based assessment of Akt inhibitors' polypharmacology. The PKIs' TFAP signatures were obtained as described by Fig. 1 legend. **A.** The TFAP signatures of GDC 0068 (in red) at indicated concentrations overlayed on the consensus Akt PKI signature (in blue). **B.** The TFAP signatures of A 674563 (in red) at indicated concentrations overlayed on the consensus Akt (upper panel) and CGK (bottom panel) PKI signatures. The similarity of the overlaid signatures calculated as Pearson correlation coefficient ***r***. Each TFAP signature is an average of three independent FACTORIAL assays.

Fig. 6. The TFAP-based assessment of ERK inhibitors' polypharmacology. The PKIs' TFAP signatures were obtained as described by Fig. 1 legend. **A.** The TFAP signatures of GDC 0094 (in red) at indicated concentrations overlayed on the consensus ERK PKI signature (at 0.03 to 2.2 uM) or the consensus signature of HDAC inhibitors (at 6.6 uM) (in blue). **B.** The TFAP signatures of Ulixertinib (in red) overlayed on the consensus ERK PKI signature (upper panel). Bottom panel: The Ulixertinib signatures (red) overlaid on the consensus signatures of Raf or mitochondria ETC inhibitors (blue). The similarity of

the overlaid signatures calculated as Pearson correlation coefficient ***r***. Each TFAP signature is an average of three independent FACTORIAL assays.

Fig. 7. Evaluating PKI chemical probes. The graphs show the similarity values (Pearson correlation ***r***) of PKI TFAP signatures vs. the consensus signatures of Akt (A) and MEK (B) inhibitors. The similarity thresholds (in grey) are set at r=0.70. The specificity windows (in green) indicate PKI concentrations for the on-target activity. Off-target concentrations are shown in red. Each graph is an average of three independent FACTORIAL assays.

Materials and Methods.

Cells and reagents. The FACTORIAL assay was conducted in HepG2 cells [American Type Culture Collection (ATCC) #HB-8065], the HG19 subclone (Attagene), which was selected for an elevated xenobiotic metabolic activity[40]. Cells were maintained in a Dulbecco's modified Eagle's medium (DMEM) growth medium supplemented with 1% charcoal-stripped fetal bovine serum and antibiotics.

Kinase inhibitors were purchased from Tocris (www.tocris.com), Selleck Chemicals (www.selleckchem.com), and Cayman Chemical (www.caymanchem.com). To avoid the possible artifacts and ensure the reproducibility of inhibitors' TFAP signatures, we evaluated different batches of kinase inhibitors from multiple vendors. All inhibitors were dissolved in dimethyl sulfoxide (DMSO). The final concentration of DMSO in cell growth medium did not exceed 0.2%.

Cell viability. Cell viability was evaluated by the XTT [2,3-bis-(2-methoxy-4-nitro-5-sulfophenyl)-2H-tetrazolium-5-carboxanilide] assay (ATCC) in HG19/HepG2 cells. As a baseline, we used cells treated with corresponding dilutions of the vehicle (DMSO).

The mitochondria function assay. To assess PKIs' effects on the mitochondria function, we used a galactose viability test in HepG2 cells[41]. These cells generate most of ATP via glycolysis and can survive mitochondrial inhibition. Substituting glucose for galactose in the growth medium inhibits glycolysis and allows detecting drug-induced mitochondrial malfunction[41].

We compared cell viability after incubation with tested compounds in glucose- or galactose-containing DMEM media. Briefly, HepG2 cells were plated in 96-well plates at 10^4 cells/well density. Twenty-four hours later, cells were rinsed twice with a glucose-free DMEM medium (Gibco, #11966-025) and incubated in a DMEM medium supplemented with 10 mM glucose or galactose and 0.1% FBS. After a 24-h treatment with tested compounds, cell viability was assessed by the XTT assay.

The FACTORIAL® assay. The FACTORIAL assay in HepG2/HG19 cells was conducted as described[11,13]. The mix of 47 RTU plasmids was transiently transfected in a suspension of assay cells using TransIT-LT1 reagent (Mirus). The transfected cells were plated into 12-well plates, each well representing an independent FACTORIAL assay. Twenty-four hours later, cells were rinsed and incubated for another 24 hours with the evaluated compounds. Total RNA was isolated, and the RTU activity profiles were assessed by consecutive steps of RT-PCR amplification, Hpa I digest, and capillary electrophoresis, as described[11,13] (Fig. S1).

TFAP signatures. Fold-change of TF transcriptional activity was calculated by dividing the RTU activity values in compound-treated cells by those in vehicle-treated cells. The TFAP signatures are shown as radial graphs with 47 axes indicating the fold changes of

corresponding RTUs on a logarithmic scale. A value of 1.0 indicated no compound's effects on the TF activity.

The pair-wise similarity of TFAP signatures was assessed as the Pearson correlation coefficient ***r***. The signatures with the similarity r>0.70 were considered identical. In addition, we calculated the Euclidean distance ***d*** from the null signature to discriminate the experimental noise. The signatures with ***d***<0.10 were considered the null signature.

Consensus PKI signatures. To identify the consensus signature for PKIs of a given kinase family, we analyzed PKIs' TFAP signatures at multiple concentrations using a recurrent agglomerative hierarchical clustering algorithm as described in our previous publication[11]. The resulting clusters contained TFAP signatures with the similarity values r exceeding the clustering threshold of 0.70. The largest cluster containing the signatures of most PKIs at multiple concentrations was considered the main cluster, and its center signature was presumed the consensus PKI signature. When in doubt, we evaluated additional PKIs to confirm the main cluster's identity.

Acknowledgements. We thank D. D. Drewry, L.M. Graves, and W. Zuercher for critique and helpful suggestions. Funding: This work was supported by NIH grants R44GM125469 and R44GM136083.
Author contributions: A.M. and S.S.M. designed the research. A.M., L.M., E.M., K.L.G., and B.L. performed the research. S.M. Jr. developed algorithms for data analysis. A.M. and S.S.M. analyzed the data. S.S.M. wrote the manuscript with input from A.M.
Competing interests: A.M., L.M., E.M., and S.S.M. have competing financial interests as Attagene employees and shareholders. A.M. and S.S.M. are inventors on a U.S. patent related to this work (no. 7,700,284, issued on 20 April 2010). The authors declare no other competing interests.
Data and materials availability: All data needed to evaluate the conclusions in the paper are present in the paper and/or the Supplementary Materials. Additional data related to this paper may be requested from the authors.

Supplementary Materials.

Fig. S1. The workflow and endpoints of the FACTORIAL assay.

Fig. S2. The TFAP signatures of Akt inhibitors.

Fig. S3. The TFAP signatures of CDK inhibitors.

Fig. S4. The TFAP signatures of Aurora inhibitors.

Fig. S5. The TFAP signatures of Raf inhibitors.

Fig. S6. The TFAP signatures of MEK inhibitors.

Fig. S7. Assessing the mitochondria function in the presence of kinase inhibitors.

Literature cited.

1. Cohen, P. Protein kinases — the major drug targets of the twenty-first century? *Nat. Rev. Drug Discov.* **1**, 309–315 (2002).
2. Cohen, P. & Alessi, D. R. Kinase drug discovery--what's next in the field? *ACS Chem. Biol.* **8**, 96–104 (2013).
3. Ferguson, F. M. & Gray, N. S. Kinase inhibitors: the road ahead. *Nat. Rev. Drug Discov.* **17**, 353–377 (2018).
4. Anastassiadis, T., Deacon, S. W., Devarajan, K., Ma, H. & Peterson, J. R. Comprehensive assay of kinase catalytic activity reveals features of kinase inhibitor selectivity. *Nat. Biotechnol.* **29**, 1039–1045 (2011).
5. Davis, M. I. *et al.* Comprehensive analysis of kinase inhibitor selectivity. *Nat. Biotechnol.* **29**, 1046–1051 (2011).
6. Médard, G. *et al.* Optimized Chemical Proteomics Assay for Kinase Inhibitor Profiling. *J. Proteome Res.* **14**, 1574–1586 (2015).
7. Krulikas, L. J. *et al.* Application of Integrated Drug Screening/Kinome Analysis to Identify Inhibitors of Gemcitabine-Resistant Pancreatic Cancer Cell Growth. *SLAS Discov. Adv. Life Sci. R&D* **23**, 850–861 (2018).
8. Huber, K. V. M. *et al.* Proteome-wide drug and metabolite interaction mapping by thermal-stability profiling. *Nat. Methods* **12**, 1055–1057 (2015).
9. Dranchak, P. *et al.* Profile of the GSK Published Protein Kinase Inhibitor Set Across ATP-Dependent and-Independent Luciferases: Implications for Reporter-Gene Assays. *PLoS One* **8**, e57888 (2013).
10. Peters, J.-U. Polypharmacology – Foe or Friend? *J. Med. Chem.* **56**, 8955–8971 (2013).
11. Medvedev, A. *et al.* Evaluating biological activity of compounds by transcription factor activity profiling. *Sci. Adv.* **4**, eaar4666 (2018).
12. Romanov, S. *et al.* Homogeneous reporter system enables quantitative functional assessment of multiple transcription factors. *Nat. Methods* **5**, 253–60 (2008).
13. Romanov, S. *et al.* Homogeneous reporter system enables quantitative functional assessment of multiple transcription factors. *Nat Methods* **5**, 253–260 (2008).
14. Richard Lowry (2012). 'Concepts and Applications of Inferential Statistics'. Available at: http://vassarstats.net/textbook/ch4apx.html.
15. Manning, B. D. & Toker, A. Leading Edge Review AKT/PKB Signaling: Navigating the Network. *Cell* **169**, 381–405 (2017).
16. Luo, Y., Shoemaker AR, Liu X, Woods KW, Thomas SA, de Jong R, Han EK, Li T, Stoll VS, Powlas JA, Oleksijew A, Mitten MJ, Shi Y, Guan R, McGonigal TP, Klinghofer V, Johnson EF, Leverson JD, Bouska JJ, Mamo M, Smith RA, Gramling-Evans EE, Zinker BA, Mika AK, G. V. Potent and selective inhibitors of Akt kinases slow the progress of tumors in vivo. *Mol. Cancer Ther.* **4**, 977–986 (2005).
17. Martorana, F. *et al.* AKT Inhibitors: New Weapons in the Fight Against Breast Cancer? *Front. Pharmacol.* **12**, (2021).
18. Fang, D. *et al.* PHOSPHORYLATION OF β-CATENIN BY AKT PROMOTES β -CATENIN TRANSCRIPTIONAL ACTIVITY. *J. Biol. Chem.* **282**, 11221 (2007).
19. Joung, S. M. *et al.* Akt Contributes to Activation of the TRIF-Dependent Signaling Pathways of TLRs by Interacting with TANK-Binding Kinase 1. *J. Immunol.* **186**, 499–507 (2011).
20. Romashkova, J. A. & Makarov, S. S. NF-kappaB is a target of AKT in anti-apoptotic PDGF signalling. *Nature* **401**, 86–90 (1999).
21. Gottlieb, T. M., Martinez Leal, J. F., Seger, R., Taya, Y. & Oren, M. Cross-talk

between Akt, p53 and Mdm2: possible implications for the regulation of apoptosis. *Oncogene 2002 218* **21**, 1299–1303 (2002).
22. Zhang, M. *et al.* CDK inhibitors in cancer therapy, an overview of recent development. *Am. J. Cancer Res.* **11**, 1913 (2021).
23. Du, R., Huang, C., Liu, K., Li, X. & Dong, Z. Targeting AURKA in Cancer: molecular mechanisms and opportunities for Cancer therapy. *Mol. Cancer* **20**, (2021).
24. Roberts, P. J. & Der, C. J. Targeting the Raf-MEK-ERK mitogen-activated protein kinase cascade for the treatment of cancer. *Oncogene* **26**, 3291–310 (2007).
25. McCubrey, J. A. *et al.* ROLES OF THE RAF/MEK/ERK PATHWAY IN CELL GROWTH, MALIGNANT TRANSFORMATION AND DRUG RESISTANCE. *Biochim. Biophys. Acta* **1773**, 1263 (2007).
26. Sun, Z., Huang, Z. & Zhang, D. D. Phosphorylation of Nrf2 at multiple sites by MAP kinases has a limited contribution in modulating the Nrf2-dependent antioxidant response. *PLoS One* **4**, (2009).
27. Parry, D. *et al.* Dinaciclib (SCH 727965), a Novel and Potent Cyclin-Dependent Kinase Inhibitor. *Mol. Cancer Ther.* **9**, 2344–2353 (2010).
28. Pennati, M. *et al.* Potentiation of paclitaxel-induced apoptosis by the novel cyclin-dependent kinase inhibitor NU6140: a possible role for survivin down-regulation. *Mol. Cancer Ther.* **4**, 1328–1337 (2005).
29. Jorda, R. *et al.* How Selective Are Pharmacological Inhibitors of Cell-Cycle-Regulating Cyclin-Dependent Kinases? *J. Med. Chem.* **61**, 9105–9120 (2018).
30. Lin, J. *et al.* Targeting activated Akt with GDC-0068, a novel selective Akt inhibitor that is efficacious in multiple tumor models. *Clin. Cancer Res.* **19**, 1760–1772 (2013).
31. Chorner, P. M. & Moorehead, R. A. A-674563, a putative AKT1 inhibitor that also suppresses CDK2 activity, inhibits human NSCLC cell growth more effectively than the pan-AKT inhibitor, MK-2206. *PLoS One* **13**, e0193344 (2018).
32. Wang, A. *et al.* Dual inhibition of AKT/FLT3-ITD by A674563 overcomes FLT3 ligand-induced drug resistance in FLT3-ITD positive AML. *Oncotarget* **7**, 29131 (2016).
33. Blake, J. F. *et al.* Discovery of (S)-1-(1-(4-Chloro-3-fluorophenyl)-2-hydroxyethyl)-4-(2-((1-methyl-1H-pyrazol-5-yl)amino)pyrimidin-4-yl)pyridin-2(1H)-one (GDC-0994), an Extracellular Signal-Regulated Kinase 1/2 (ERK1/2) Inhibitor in Early Clinical Development. *J. Med. Chem.* **59**, 5650–5660 (2016).
34. Sullivan, R. J. *et al.* First-in-Class ERK1/2 Inhibitor Ulixertinib (BVD-523) in Patients with MAPK Mutant Advanced Solid Tumors: Results of a Phase I Dose-Escalation and Expansion Study. *Cancer Discov.* **8**, 184–195 (2018).
35. Arrowsmith, C. H. *et al.* The promise and peril of chemical probes. *Nat. Chem. Biol.* **11**, 536–41 (2015).
36. Sweis, R. F. Target (In)Validation: A Critical, Sometimes Unheralded, Role of Modern Medicinal Chemistry. *ACS Med. Chem. Lett.* **6**, 618–621 (2015).
37. Garbaccio, R. M. & Parmee, E. R. The Impact of Chemical Probes in Drug Discovery: A Pharmaceutical Industry Perspective. *Cell Chem. Biol.* **23**, 10–17 (2016).
38. Blagg, J. & Workman, P. Choose and Use Your Chemical Probe Wisely to Explore Cancer Biology. *Cancer Cell* **32**, (2017).
39. Welcome to the Chemical Probes Portal. Available at: https://www.chemicalprobes.org/. (Accessed: 28th February 2022)
40. Martin, M. T. *et al.* Impact of environmental chemicals on key transcription regulators and correlation to toxicity end points within EPA's ToxCast program.

Chem Res Toxicol **23**, 578–590 (2010).
41. Marroquin, L. D., Hynes, J., Dykens, J. A., Jamieson, J. D. & Will, Y. Circumventing the Crabtree effect: replacing media glucose with galactose increases susceptibility of HepG2 cells to mitochondrial toxicants. *Toxicol. Sci.* **97**, 539–47 (2007).

A AKT

PKI	Target	MOA	[C], uM	Corr. *r*
Afuresertib	pan-AKT	ATP	0.25	**0.94**
AZD 5363	pan-AKT	ATP	0.06	**0.89**
GDC-0068	pan-AKT	ATP	0.19	**0.90**
GSK690693	pan-AKT	ATP	0.74	**0.86**
MK-2206	AKT 2,3	Allost.	2.20	**0.79**

B CDK

PKI	Target	MOA	[C], uM	Corr., r
(R)-Roscovitine	CDK1/2/5/7/9	ATP	20.00	**0.83**
AT7519	CDK 1/2/4/6/9	ATP	0.25	**0.87**
AZD 5438	CDK 1/2/9	ATP	2.20	**0.76**
BMS-265246	CDK 1/2	ATP	1.70	**0.9**
Cdk2 Inhibitor II	CDK 2	ATP	2.20	**0.74**
Dinaciclib	CDK2/5/1/9	ATP	0.03	**0.88**
DRB	CDK7/8/9 and CKII	ATP	20.00	**0.86**
Flavopiridol	CDK 1/2/4/6	ATP	0.25	**0.92**
NU 6140	CDK2, Aurora B/A	ATP	6.70	**0.79**
PD 0332991	CDK 4/6	ATP	15.00	**0.82**
Purvalanol A	CDK 1/2/5	ATP	6.70	**0.76**
R547	CDK 1/2/4	ATP	1.70	**0.82**
SU 9516	CDK 1/2/4	ATP	15.00	**0.88**

C Aurora

PKI	Target	MOA	[C], uM	Corr., *r*
Alisertib	Aurora A	ATP	15	**0.88**
CCT137690	Aurora A/B	ATP	0.2	**0.85**
PF-03814735	Aurora A/B	ATP	0.1	**0.89**
Tozasertib	Aurora A/C/B	ATP	2.2	**0.88**
ZM 447439	Aurora B/C/A	ATP	2.2	**0.85**

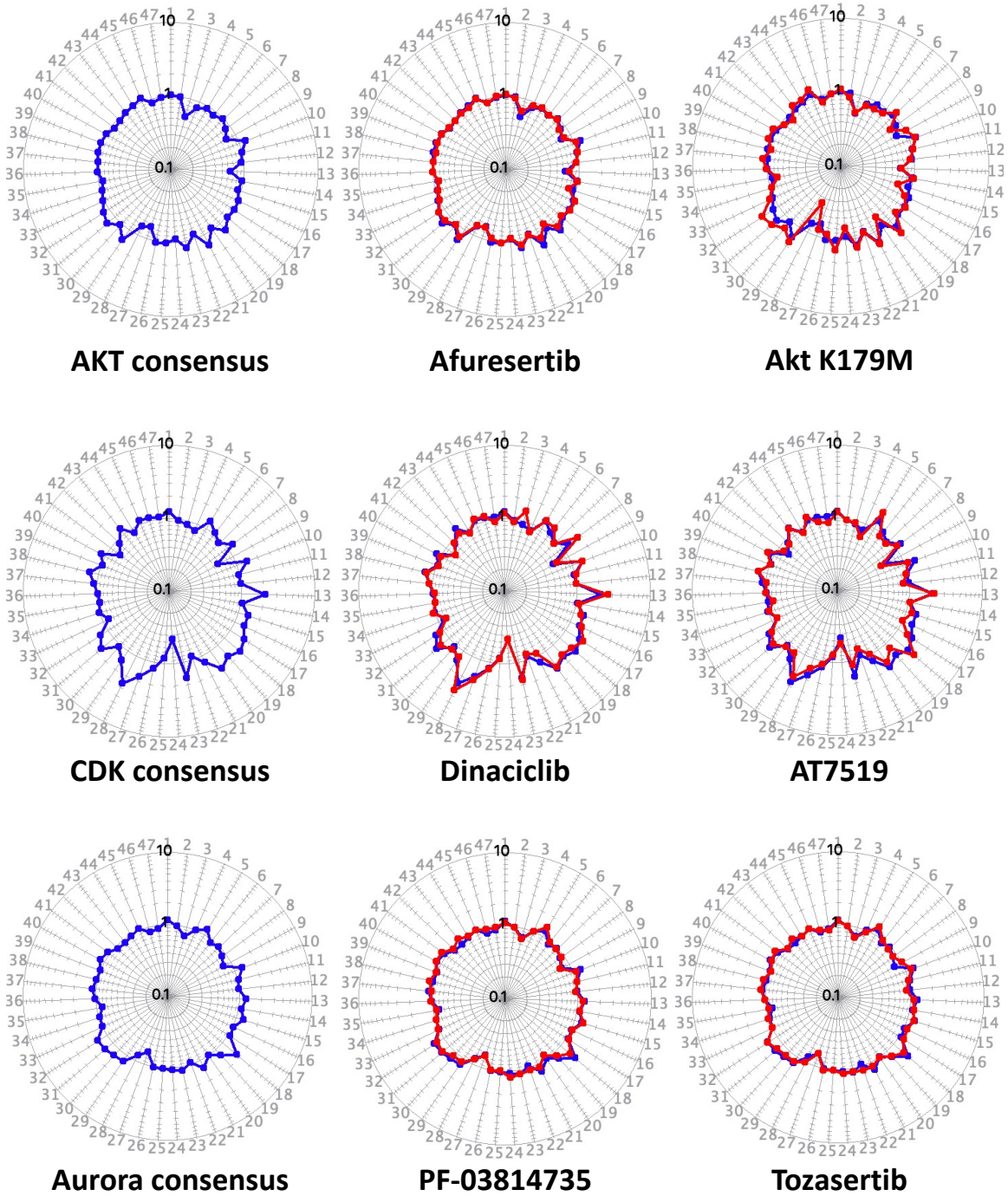

RTU #	Name
1	TGFRE
2	HNF6
3	TCF
4	Ebox
5	PPAR
6	NF1
7	GR
8	AP-1
9	ISRE
10	MTF-1
11	STAT3
12	TAL
13	NF-κB
14	FoxA2
15	CMV
16	Xbp1
17	CREB
18	AhR
19	EGR
20	NRF2
21	TA
22	ER
23	Oct
24	LXR
25	HSF-1
26	SREBP
27	p53
28	BMPRE
29	Pax6
30	HIF-1α
31	VDR
32	ROR
33	Ets
34	GLI-1
35	NRF1
36	GATA
37	E2F
38	C/EBP
39	Myb
40	PBREM
41	FXR
42	AP-2
43	RAR
44	FoxO
45	SOX
46	Sp1
47	Myc

Figure 1

A Raf

PKI	Target	MOA	[C], uM	Corr., *r*
AZ 628	pan-Raf	ATP	60.00	**0.91**
Encorafenib	B-Raf	ATP	2.20	**0.88**
PLX4720	B-Raf	ATP	60.00	**0.74**
RAF265	pan-Raf	ATP	0.74	**0.95**
Regorafenib	pan-Raf multikinase	ATP	0.27	**0.87**
Sorafenib	pan-Raf multikinase	ATP	0.27	**0.77**
Vemurafenib	pan-Raf multikinase	ATP	6.67	**0.83**

B MEK

PKI	Target	MOA	[C], uM	Corr., *r*
Consensus				**1.00**
Binimetinib	MEK1/2	Allost.	2.2	**0.95**
PD 0325901	MEK1/2	Allost.	5	**0.70**
Pimasertib	MEK1/2	Allost.	0.005	**0.83**
Selumetinib	MEK1,ERK1/2	Allost.	0.24	**0.95**
Trametinib	MEK1/2	Allost.	0.24	**0.98**
U0126	MEK1/2	Allost.	0.33	**0.75**

C ERK

PKI	Target	MOA	[C], uM	Corr., *r*
GDC-0994	ERK1/2	ATP	0.027	0.93
Ulixertinib	ERK1/2	ATP	0.027	0.90

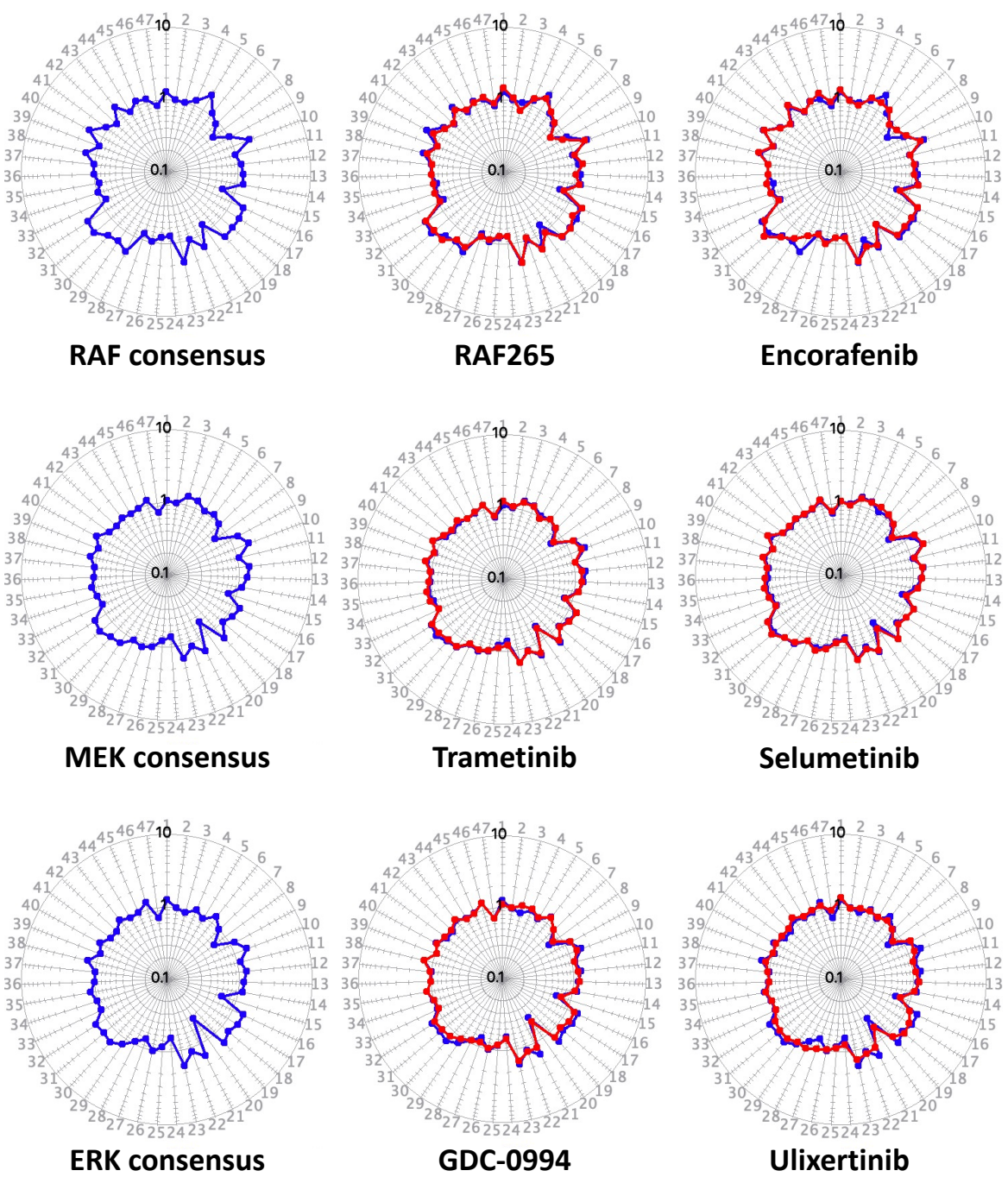

RTU #	Name
1	TGFRE
2	HNF6
3	TCF
4	Ebox
5	PPAR
6	NF1
7	GR
8	AP-1
9	ISRE
10	MTF-1
11	STAT3
12	TAL
13	NF-κB
14	FoxA2
15	CMV
16	Xbp1
17	CREB
18	AhR
19	EGR
20	NRF2
21	TA
22	ER
23	Oct
24	LXR
25	HSF-1
26	SREBP
27	p53
28	BMPRE
29	Pax6
30	HIF-1α
31	VDR
32	ROR
33	Ets
34	GLI-1
35	NRF1
36	GATA
37	E2F
38	C/EBP
39	Myb
40	PBREM
41	FXR
42	AP-2
43	RAR
44	FoxO
45	SOX
46	Sp1
47	Myc

Figure 2

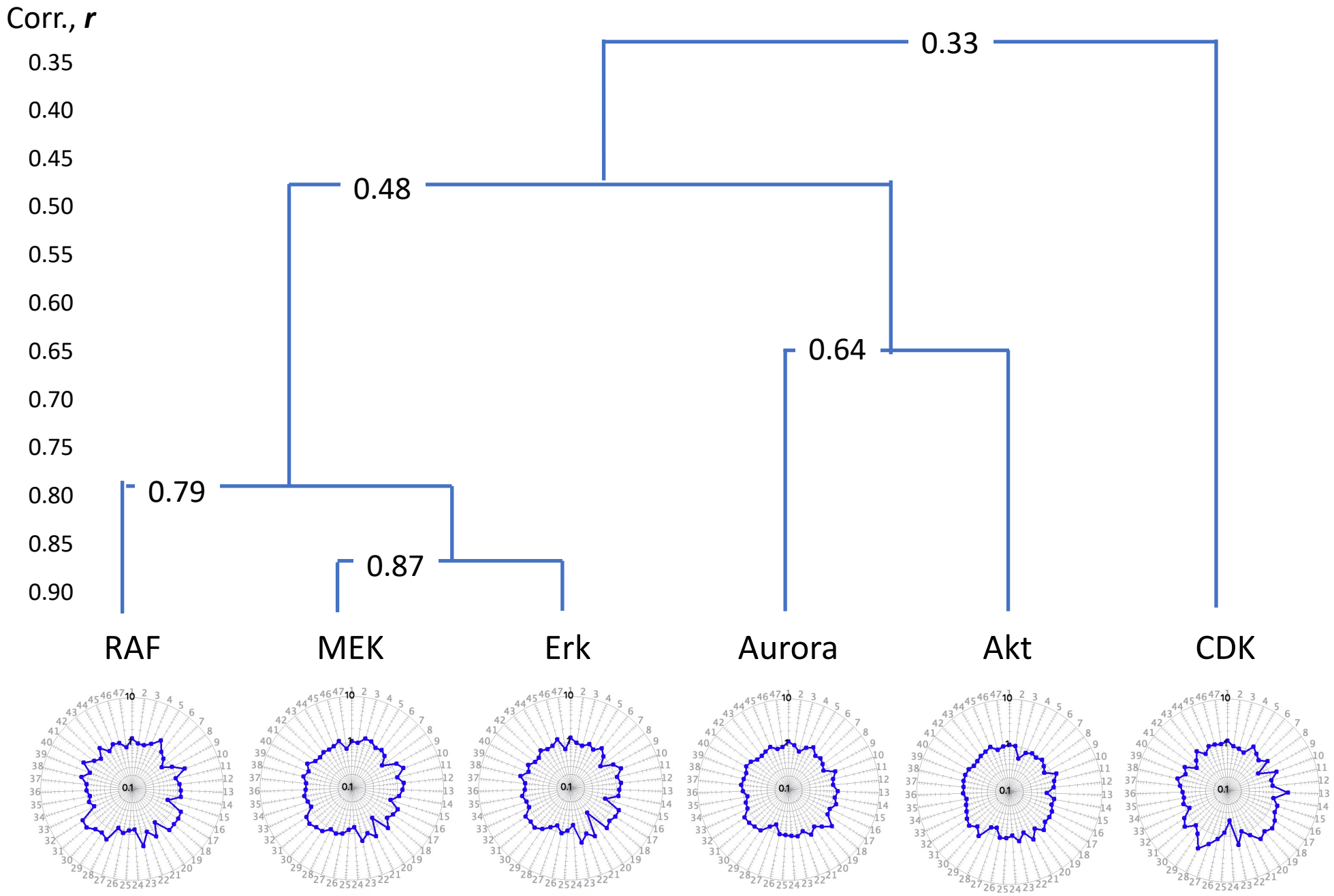
Corr., r
0.35
0.40
0.45
0.50
0.55
0.60
0.65
0.70
0.75
0.80
0.85
0.90
0.33
0.48
0.64
0.79
0.87
RAF
MEK
Erk
Aurora
Akt
CDK

Figure 3

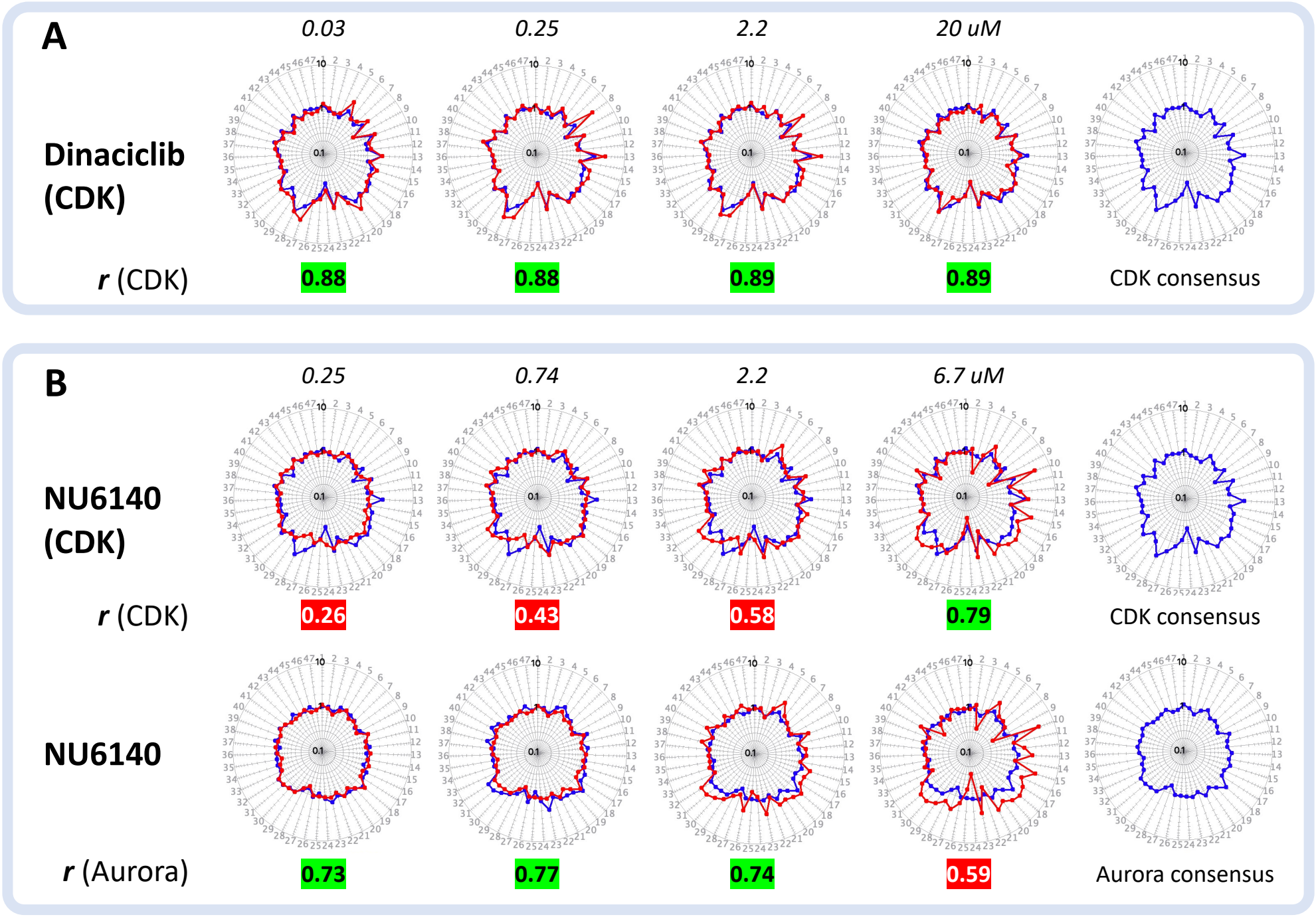
A
0.03
0.25
2.2
20 uM
Dinaciclib (CDK)
r (CDK)
0.88
0.88
0.89
0.89
CDK consensus
B
0.25
0.74
2.2
6.7 uM
NU6140 (CDK)
r (CDK)
0.26
0.43
0.58
0.79
CDK consensus
NU6140
r (Aurora)
0.73
0.77
0.74
0.59
Aurora consensus

Figure 4

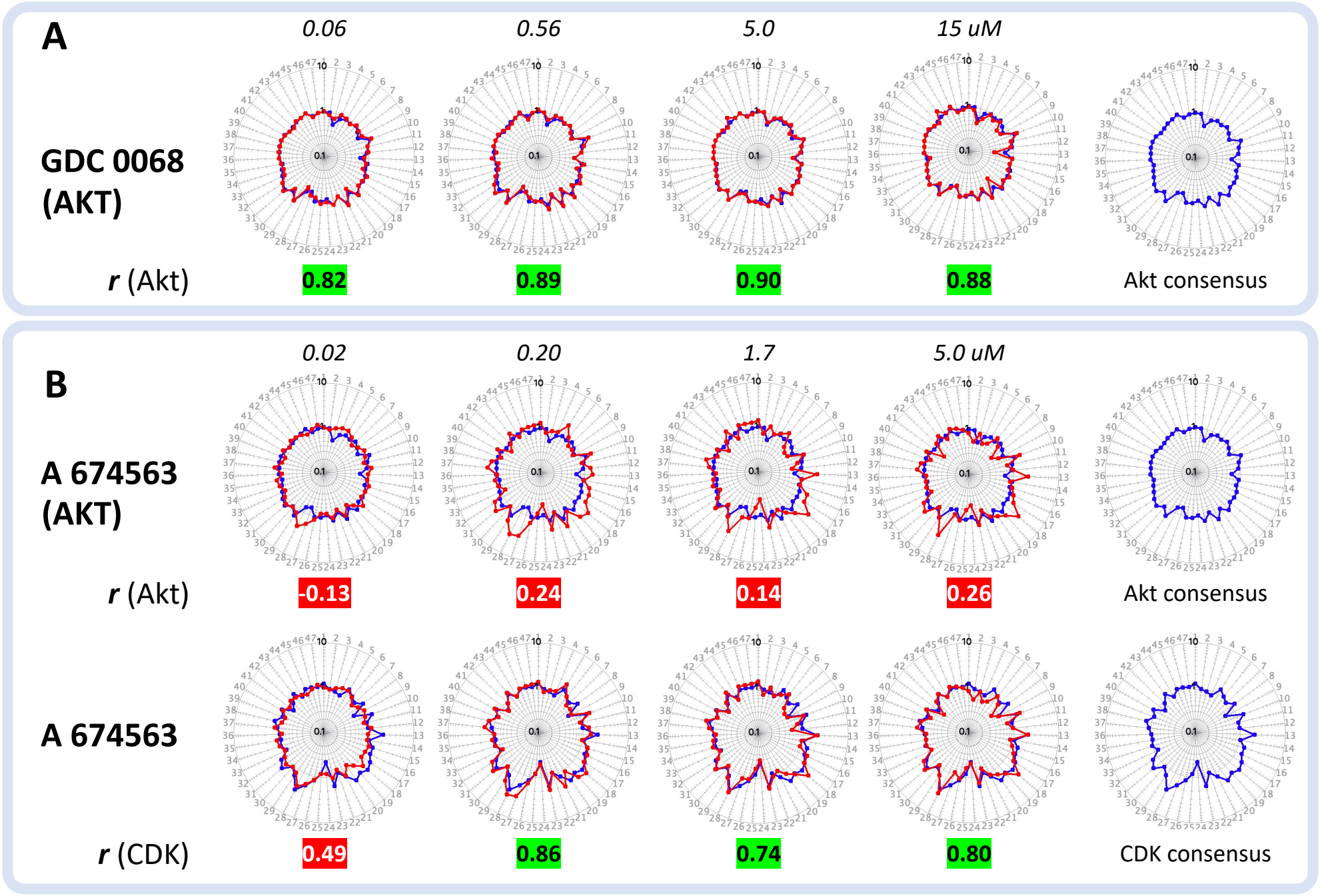
A
0.06
0.56
5.0
15 uM
GDC 0068 (AKT)
r (Akt)
0.82
0.89
0.90
0.88
Akt consensus
B
0.02
0.20
1.7
5.0 uM
A 674563 (AKT)
r (Akt)
-0.13
0.24
0.14
0.26
Akt consensus
A 674563
r (CDK)
0.49
0.86
0.74
0.80
CDK consensus

Figure 5

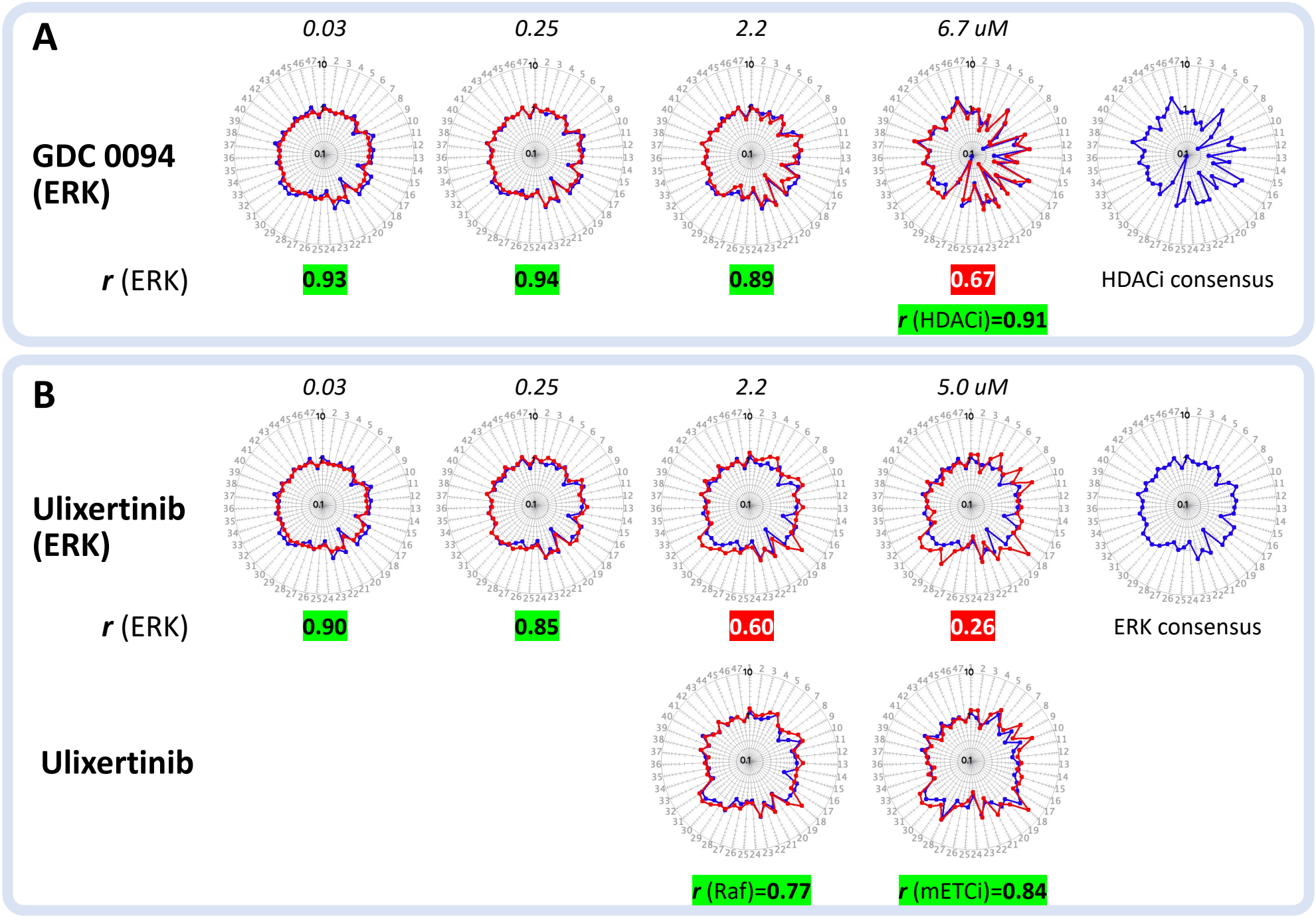
A
0.03
0.25
2.2
6.7 uM
GDC 0094 (ERK)
r (ERK)
0.93
0.94
0.89
0.67
HDACi consensus
r (HDACi)=0.91
B
0.03
0.25
2.2
5.0 uM
Ulixertinib (ERK)
r (ERK)
0.90
0.85
0.60
0.26
ERK consensus
Ulixertinib
r (Raf)=0.77
r (mETCi)=0.84

Figure 6

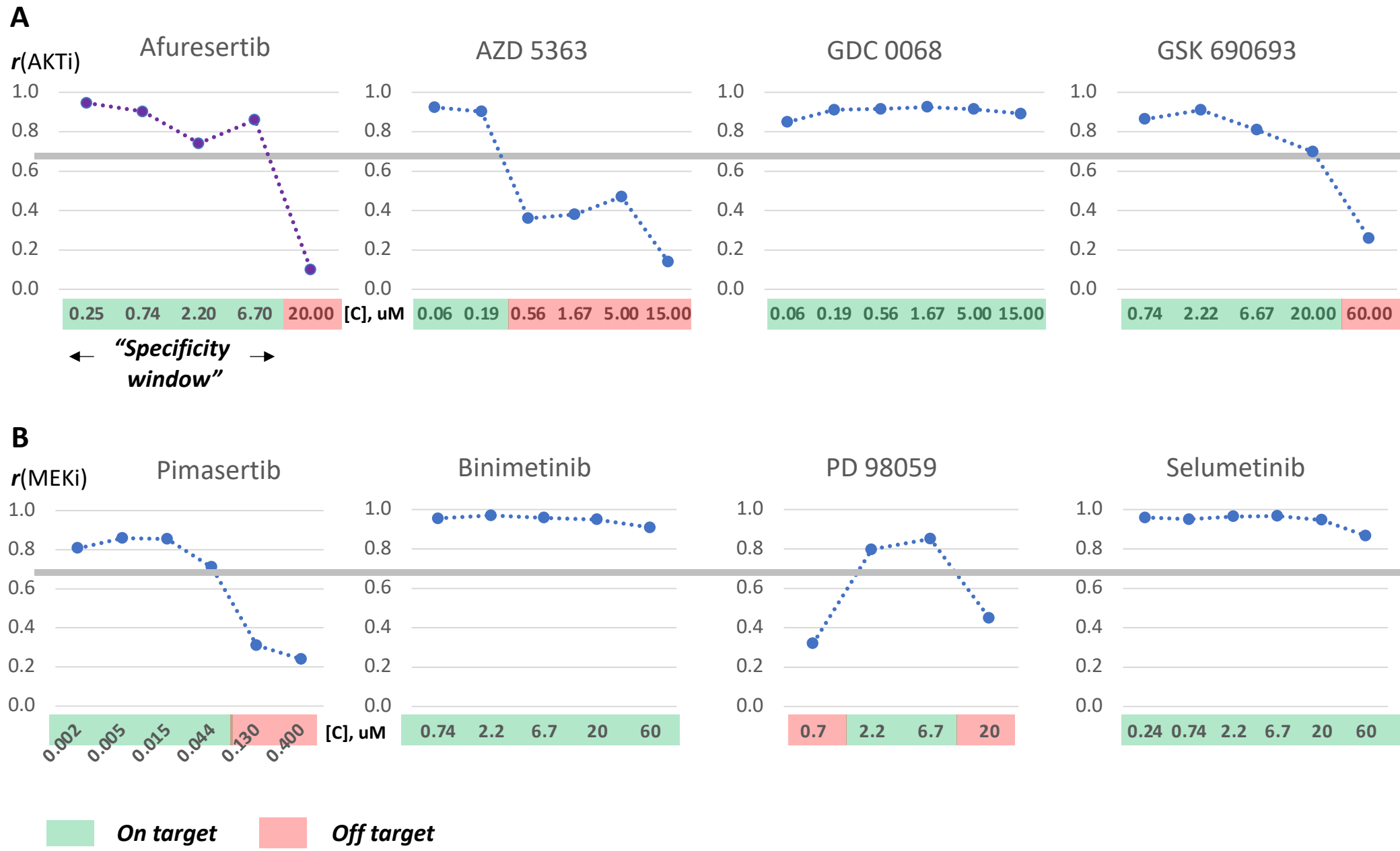
A
r(AKTi)
Afuresertib
AZD 5363
GDC 0068
GSK 690693
1.0
0.8
0.6
0.4
0.2
0.0
0.25 0.74 2.20 6.70 20.00
[C], uM
0.06 0.19 0.56 1.67 5.00 15.00
0.06 0.19 0.56 1.67 5.00 15.00
0.74 2.22 6.67 20.00 60.00
"Specificity window"
B
r(MEKi)
Pimasertib
Binimetinib
PD 98059
Selumetinib
0.002 0.005 0.015 0.044 0.130 0.400
[C], uM
0.74 2.2 6.7 20 60
0.7 2.2 6.7 20
0.24 0.74 2.2 6.7 20 60
On target
Off target

Figure 7

SUPPLEMENTARY MATERIALS

A

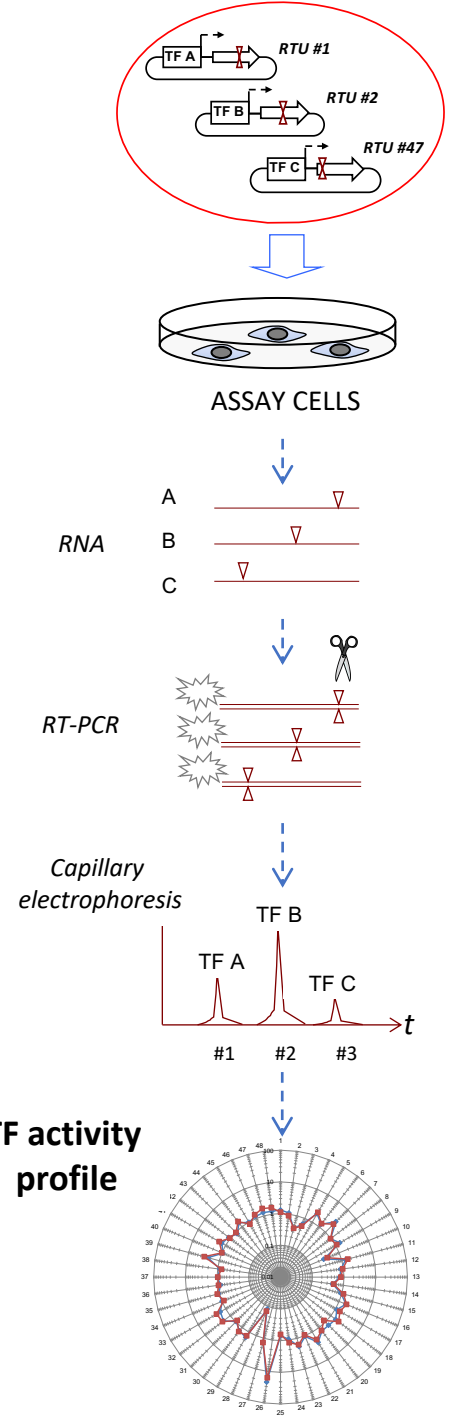

B

RTU #	Name	Transcription Factor
1	TGFRE	TGF beta response element (SMAD3/4)
2	HNF6	Hepatocyte nuclear factor 6
3	TCF	TCF/LEF
4	Ebox	Myc and Upstream Stimulatory Factor 1 (USF-1)
5	PPAR	Peroxisome proliferator activating receptor
6	NF1	Nuclear factor 1
7	GR	Glucocorticoid receptor
8	AP-1	Activator protein 1
9	ISRE	Interferon regulatory factors IRF1, IFR3
10	MTF-1	The metal regulatory transcription factor 1 (MTF-1)
11	STAT3	Signal transducer and activator of transcription 3
12	TAL	*a minimal promoter*
13	NF-κB	Nuclear factor kappa B
14	FoxA2	Forkhead box protein A2
15	CMV	Cytomegalovirus promoter-enhancer
16	Xbp1	X-Box protein 1
17	CREB	cAMP-response element binding protein
18	AhR	Aryl hydrocarbon receptor
19	EGR	Early growth response protein 1
20	NRF2	Nuclear factor (erythroid-derived 2)-like 2
21	TA	*a minimal promoter*
22	ER	Estrogen Receptor
23	Oct	Octamer transcription factor
24	LXR	Liver X receptor
25	HSF-1	Heat shock factor -1 protein
26	SREBP	Sterol Regulatory Element-Binding Protein
27	p53	The p53 transcription factor
28	BMPRE	Bone morphogenetic protein response element (SMAD4/5)
29	Pax6	Transcription factor paired box 6
30	HIF-1α	Hypoxia-inducible factor-1 alpha
31	VDR	Vitamin D receptor
32	ROR	Retinoic acid receptor -related orphan receptor protein
33	Ets	E-twenty six transcription factor
34	GLI-1	Gli-1 transcription factor
35	NRF1	Nuclear respiratory factor 1
36	GATA	GATA transcription factor
37	E2F	E2F transcription factor
38	C/EBP	The CCAAT-enhancer-binding protein
39	Myb	transcriptional activator Myb
40	PBREM	Phenobarbital responsive enhancer module /constitutive androstane receptor
41	FXR	Farnesoid X receptor
42	AP-2	Activating protein 2
43	RAR	Retinoic acid receptor
44	FoxO	Forkhead box proteins FOXO1 and FOXO3
45	SOX	SOX transcription factor
46	Sp1	Sp1 transcription factor
47	Myc	Myc transcription factor

Figure S1

A AKT

PKI	Target	MOA	[C], uM	Corr. *r*
Afuresertib	pan-AKT	ATP	0.25	**0.94**
			0.74	**0.88**
			2.22	**0.74**
			6.67	**0.85**
AZD 5363	pan-AKT	ATP	0.06	**0.89**
			0.19	**0.88**
GDC-0068	pan-AKT	ATP	0.06	**0.83**
			0.19	**0.90**
			0.56	**0.90**
			1.67	**0.91**
			5.00	**0.90**
			15.00	**0.88**
GSK690693	pan-AKT	ATP	0.74	**0.86**
			2.22	**0.92**
			6.67	**0.81**
			20.00	**0.71**
MK-2206	AKT 2,3	Allost.	2.20	**0.79**
			6.70	**0.79**
			20.00	**0.73**

B

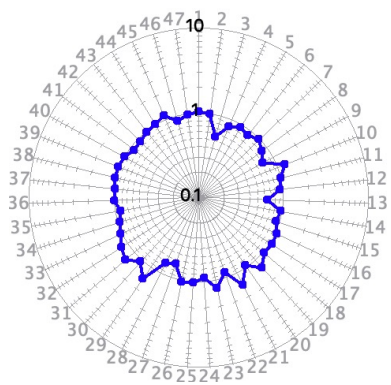

AKT consensus

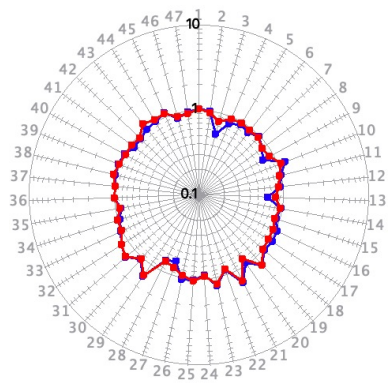

AZD5363 0.19 uM
r=0.88

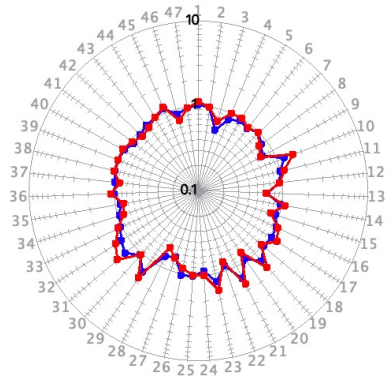

GDC0068 0.56 uM
r=0.90

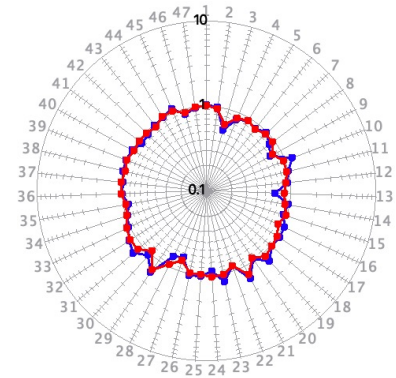

GSK690693 0.74 uM
r=0.86

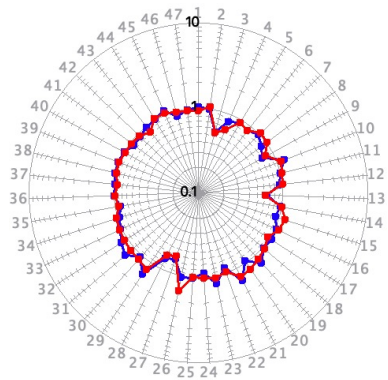

MK2206 6.7 uM
r=0.79

RTU #	Name
1	TGFRE
2	HNF6
3	TCF
4	Ebox
5	PPAR
6	NF1
7	GR
8	AP-1
9	ISRE
10	MTF-1
11	STAT3
12	TAL
13	NF-κB
14	FoxA2
15	CMV
16	Xbp1
17	CREB
18	AhR
19	EGR
20	NRF2
21	TA
22	ER
23	Oct
24	LXR
25	HSF-1
26	SREBP
27	p53
28	BMPRE
29	Pax6
30	HIF-1α
31	VDR
32	ROR
33	Ets
34	GLI-1
35	NRF1
36	GATA
37	E2F
38	C/EBP
39	Myb
40	PBREM
41	FXR
42	AP-2
43	RAR
44	FoxO
45	SOX
46	Sp1
47	Myc

Figure S2

CDK

A

Sample	Conc.	Corr. r
(R)-Roscovitine	20.00	0.83
(R)-Roscovitine	60.00	0.82
A-674563	0.19	0.84
A-674563	0.56	0.85
A-674563	1.67	0.80
A-674563	5.00	0.79
AT7519	0.25	0.87
AT7519	0.60	0.82
AT7519	0.74	0.90
AT7519	2.20	0.84
AZD 5438	2.22	0.76
AZD 5438	6.67	0.70
AZD 5438	20.00	0.73
BMS-265246	1.67	0.90
BMS-265246	5.00	0.85
Cdk2 Inhibitor II	2.20	0.74
Cdk2 Inhibitor II	6.70	0.76
Cdk2 Inhibitor II	60.00	0.74
Dinaciclib	0.03	0.88
Dinaciclib	0.08	0.91
Dinaciclib	0.24	0.88
Dinaciclib	0.74	0.88
Dinaciclib	2.20	0.89
Dinaciclib	6.70	0.93
Dinaciclib	20.00	0.89
Dinaciclib	60.00	0.73
DRB	20.00	0.86
DRB	30.00	0.84
DRB	60.00	0.90
Flavopiridol	0.07	0.78
Flavopiridol	0.22	0.72
Flavopiridol	0.25	0.92
Flavopiridol	0.67	0.83
Flavopiridol	0.74	0.91
Flavopiridol	2.00	0.85
Flavopiridol	2.20	0.87
Flavopiridol	6.70	0.75
Flavopiridol	20.00	0.75
NU 6140	6.70	0.79
PD 0332991	15.00	0.82
Purvalanol A	6.70	0.76
Purvalanol A	20.00	0.74
R547	0.56	0.70
R547	1.67	0.82
R547	5.00	0.78
R547	15.00	0.77
SU 9516	15.00	0.88

B

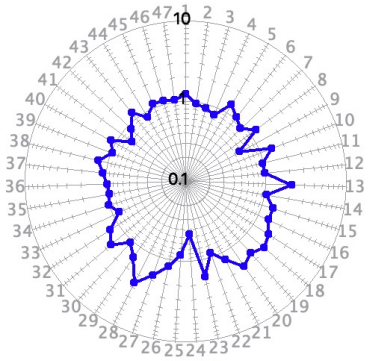

CDK consensus

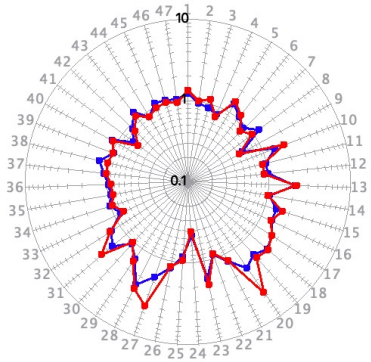

(R)-Roscovitine 20 uM
r=0.83

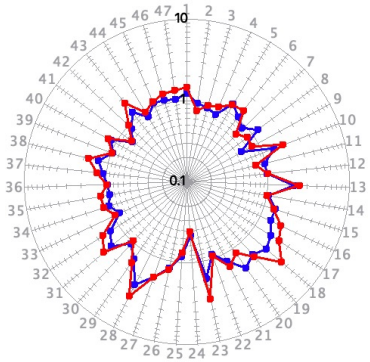

A 674563 0.56 uM
r=0.85

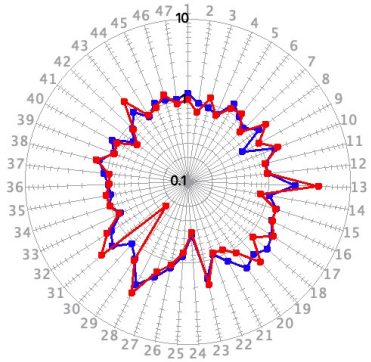

AZD 5438 20 uM
r=0.73

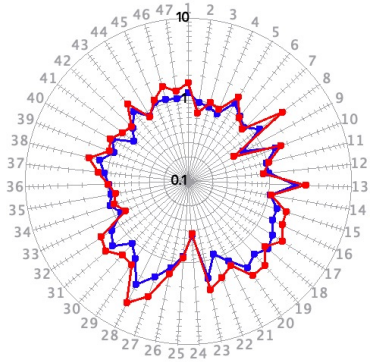

BMS 265246 5 uM
r=0.85

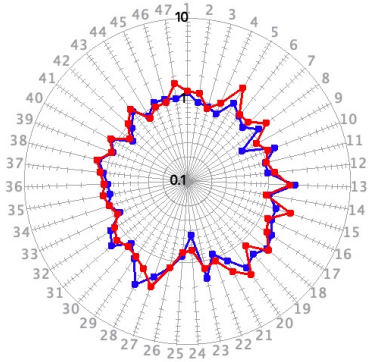

CDK2 inhibitor II 6.7 uM
r=0.0.76

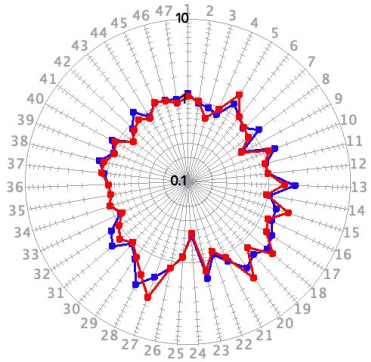

DRB 20 uM
r=0.86

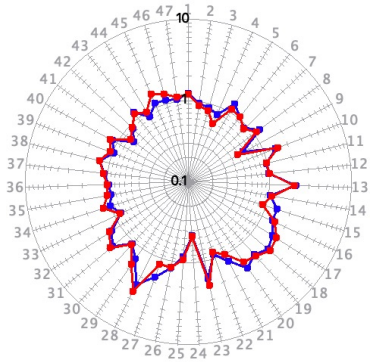

Flavopiridol 0.25 uM
r=0.92

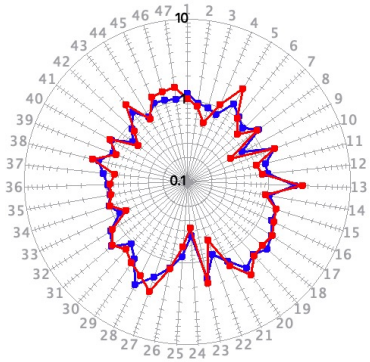

SU 9516 15 uM
r=0.88

RTU #	Name
1	TGFRE
2	HNF6
3	TCF
4	Ebox
5	PPAR
6	NF1
7	GR
8	AP-1
9	ISRE
10	MTF-1
11	STAT3
12	TAL
13	NF-κB
14	FoxA2
15	CMV
16	Xbp1
17	CREB
18	AhR
19	EGR
20	NRF2
21	TA
22	ER
23	Oct
24	LXR
25	HSF-1
26	SREBP
27	p53
28	BMPRE
29	Pax6
30	HIF-1α
31	VDR
32	ROR
33	Ets
34	GLI-1
35	NRF1
36	GATA
37	E2F
38	C/EBP
39	Myb
40	PBREM
41	FXR
42	AP-2
43	RAR
44	FoxO
45	SOX
46	Sp1
47	Myc

Figure S3

A

Aurora

PKI	C, uM	Corr. r
Consensus		1
Alisertib	15	0.875
Alisertib	5	0.834
Alisertib	1.7	0.761
CCT137690	0.2	0.845
CCT137690	0.6	0.841
CCT137690	1.7	0.787
CCT137690	5	0.758
PF-03814735	0.04	0.86
PF-03814735	0.1	0.892
PF-03814735	0.3	0.835
PF-03814735	1	0.784
PF-03814735	0.01	0.718
PF-03814735	3	0.713
Tozasertib	2.2	0.875
Tozasertib	0.74	0.854
Tozasertib	0.25	0.798
Tozasertib	6.7	0.75
ZM 447439	2.2	0.851
ZM 447439	0.25	0.819
ZM 447439	20	0.787
ZM 447439	6.7	0.776
ZM 447439	0.74	0.723

B

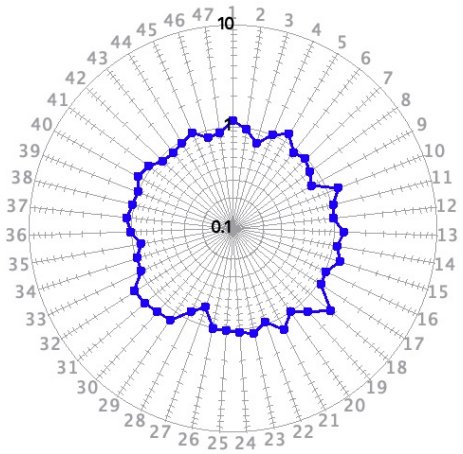

Aurora consensus

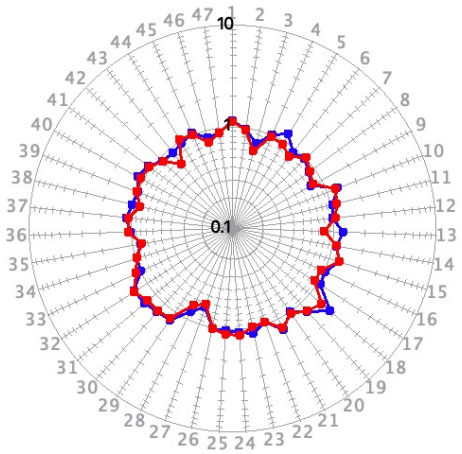

Allsertib 5 uM
r=0.83

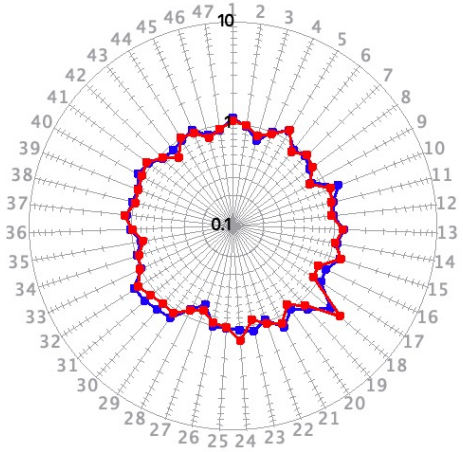

CCT137690 0.6 uM
r=0.84

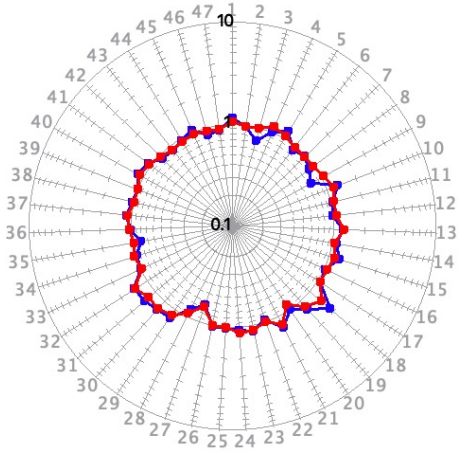

ZM447439 2.2 uM
r=0.85

RTU #	Name
1	TGFRE
2	HNF6
3	TCF
4	Ebox
5	PPAR
6	NF1
7	GR
8	AP-1
9	ISRE
10	MTF-1
11	STAT3
12	TAL
13	NF-κB
14	FoxA2
15	CMV
16	Xbp1
17	CREB
18	AhR
19	EGR
20	NRF2
21	TA
22	ER
23	Oct
24	LXR
25	HSF-1
26	SREBP
27	p53
28	BMPRE
29	Pax6
30	HIF-1α
31	VDR
32	ROR
33	Ets
34	GLI-1
35	NRF1
36	GATA
37	E2F
38	C/EBP
39	Myb
40	PBREM
41	FXR
42	AP-2
43	RAR
44	FoxO
45	SOX
46	Sp1
47	Myc

Figure S5

A

Raf

PKI	Conc., uM	Corr., r
Consensus		1.00
AZ 628	60	0.91
Encorafenib	2.2	0.88
Encorafenib	6.7	0.83
Encorafenib	0.74	0.76
Encorafenib	60	0.75
Encorafenib	20	0.73
PLX4720	60	0.74
RAF265	2.2	0.95
RAF265	0.74	0.95
RAF265	6.7	0.93
RAF265	0.25	0.93
RAF265	20	0.92
RAF265	60	0.90
RAF265	0.082	0.73
Regorafenib	0.27	0.87
Regorafenib	0.82	0.84
Regorafenib	2.47	0.76
Sorafenib	0.27	0.77
Sorafenib	0.82	0.73
Vemurafenib	6.67	0.83

B

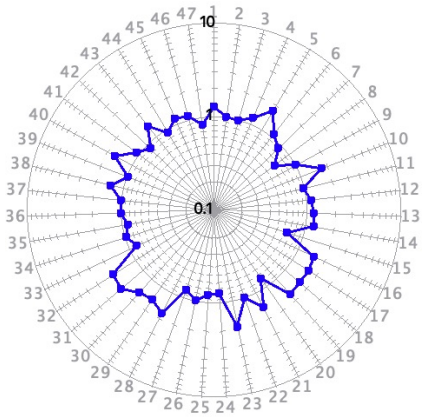

Raf consensus

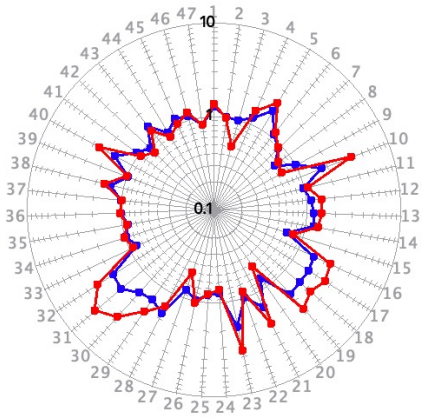

AZD 628 60 uM
r=0.91

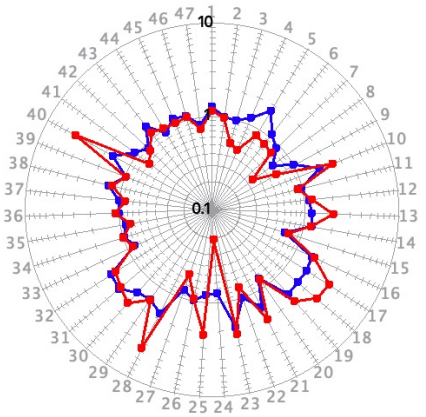

PLX 4720 60 uM
r=0.74

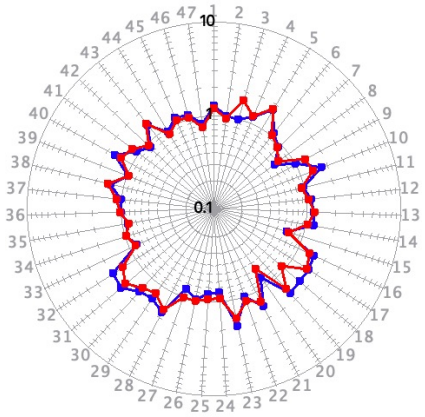

Regorafenib 0.82 uM
r=0.84

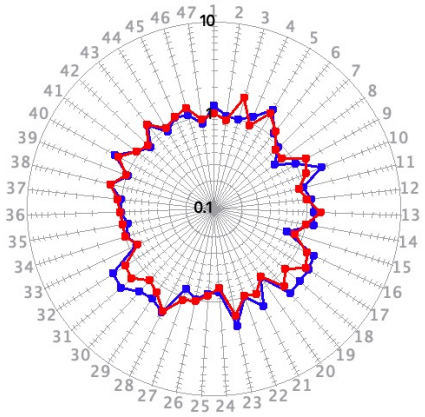

Sorafenib 0.82 uM
r=0.73

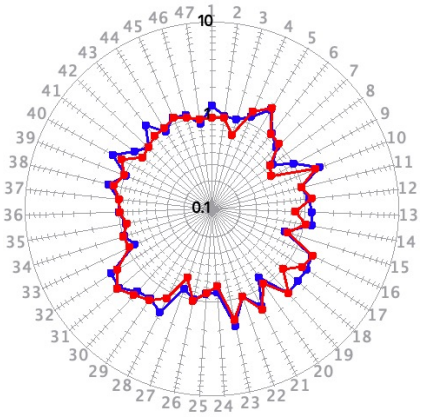

Vemurafenib 6.7 uM
r=0.83

RTU #	Name
1	TGFRE
2	HNF6
3	TCF
4	Ebox
5	PPAR
6	NF1
7	GR
8	AP-1
9	ISRE
10	MTF-1
11	STAT3
12	TAL
13	NF-κB
14	FoxA2
15	CMV
16	Xbp1
17	CREB
18	AhR
19	EGR
20	NRF2
21	TA
22	ER
23	Oct
24	LXR
25	HSF-1
26	SREBP
27	p53
28	BMPRE
29	Pax6
30	HIF-1α
31	VDR
32	ROR
33	Ets
34	GLI-1
35	NRF1
36	GATA
37	E2F
38	C/EBP
39	Myb
40	PBREM
41	FXR
42	AP-2
43	RAR
44	FoxO
45	SOX
46	Sp1
47	Myc

Figure S5

A

MEK

PKI	[C]. uM	Corr. r
Consensus		1.00
Binimetinib	60	0.97
Binimetinib	20	0.96
Binimetinib	2.2	0.95
Binimetinib	6.7	0.93
Binimetinib	0.74	0.92
Binimetinib	0.24	0.88
PD 0325901	20	0.70
PD 0325901	5	0.70
PD 98059	6.7	0.77
PD 98059	2.2	0.72
Pimasertib	0.005	0.83
Pimasertib	0.015	0.74
Pimasertib	0.002	0.73
Pimasertib	0.24	0.72
Selumetinib	20	0.97
Selumetinib	6.7	0.96
Selumetinib	0.74	0.95
Selumetinib	0.24	0.95
Selumetinib	2.2	0.94
Selumetinib	60	0.92
Trametinib	0.24	0.98
Trametinib	0.74	0.97
Trametinib	2.2	0.94
Trametinib	6.7	0.83
Trametinib	60	0.72
Trametinib	20	0.71
U0126	0.33	0.75
U0126	0.11	0.74

B

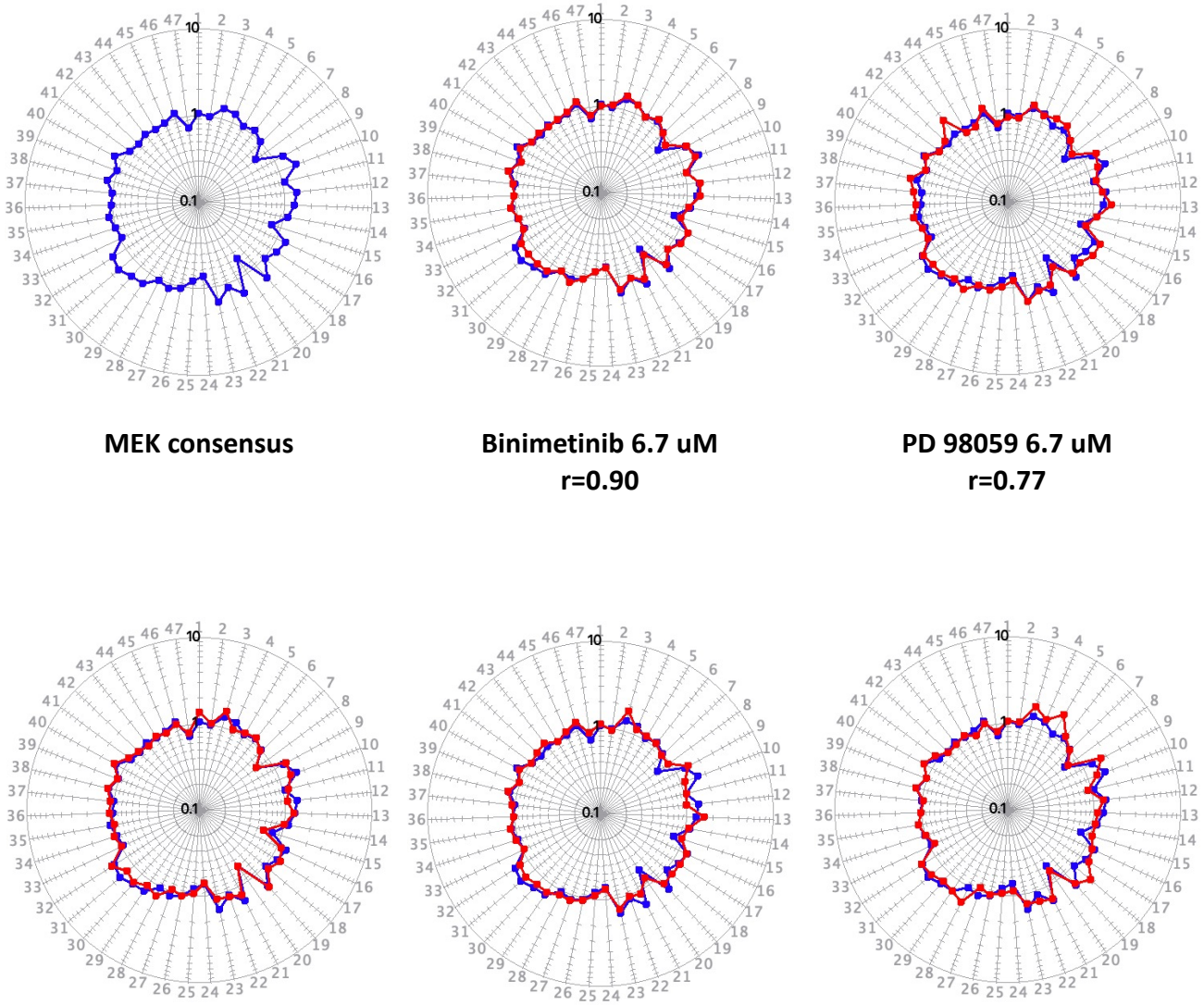

RTU #	Name
1	TGFRE
2	HNF6
3	TCF
4	Ebox
5	PPAR
6	NF1
7	GR
8	AP-1
9	ISRE
10	MTF-1
11	STAT3
12	TAL
13	NF-κB
14	FoxA2
15	CMV
16	Xbp1
17	CREB
18	AhR
19	EGR
20	NRF2
21	TA
22	ER
23	Oct
24	LXR
25	HSF-1
26	SREBP
27	p53
28	BMPRE
29	Pax6
30	HIF-1α
31	VDR
32	ROR
33	Ets
34	GLI-1
35	NRF1
36	GATA
37	E2F
38	C/EBP
39	Myb
40	PBREM
41	FXR
42	AP-2
43	RAR
44	FoxO
45	SOX
46	Sp1
47	Myc

Figure S6

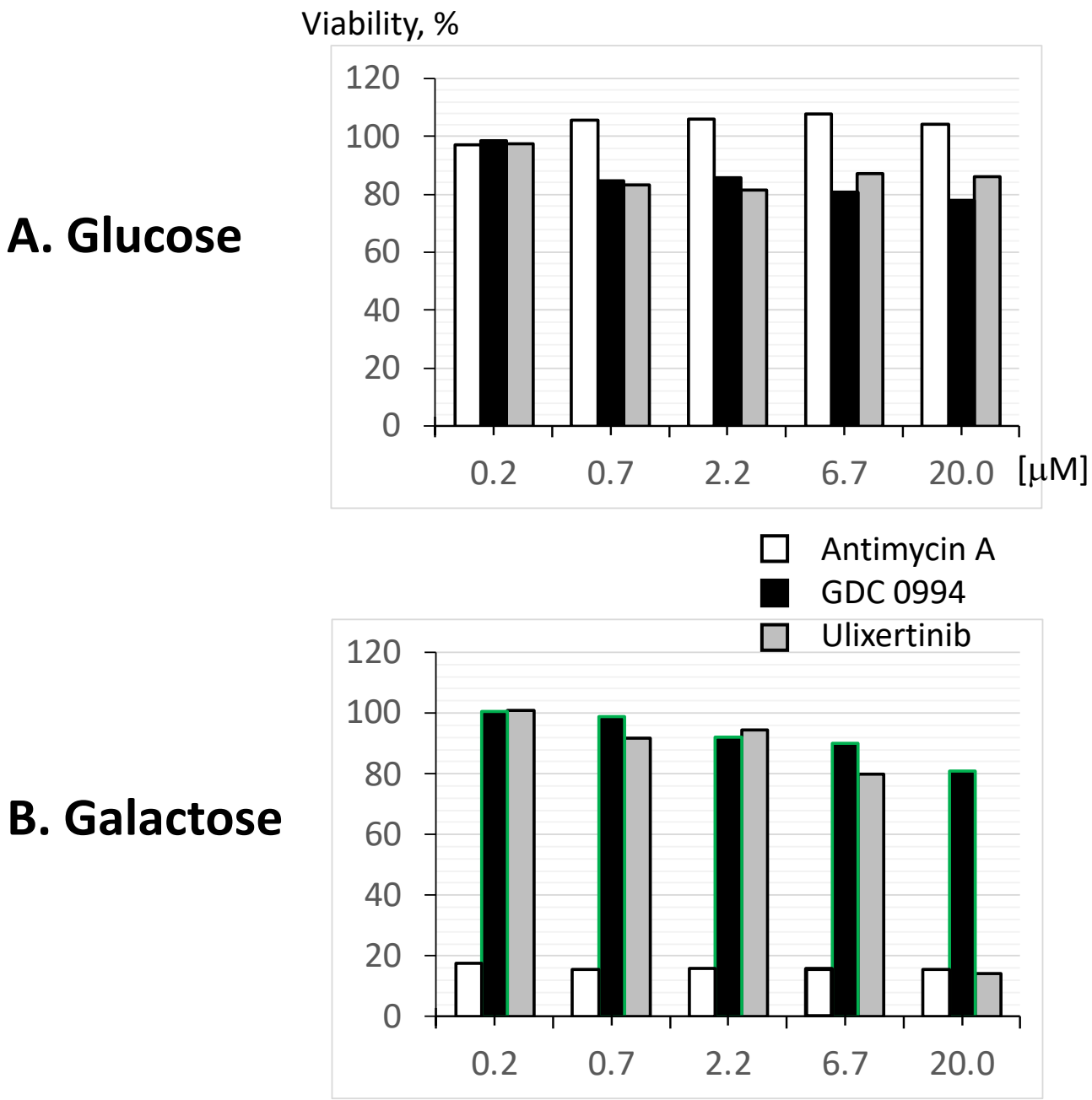

The PKIs' effects on the mitochondria function were assessed by comparing HepG2 cell viability in the presence of indicated compounds at indicated concentrations in glucose- (A) or galactose (B)-containing growth media (see *Methods*). A mitochondria inhibitor Antimycin provided a positive control.

Figure S7